Artificial Neural Network Based SGSC Scheme of DFIG For The Compensation of Grid Voltage Unbalance

S.Prasanth Kumar[1], C.Prashanth Sai[2]
[2] Assistant professor
[1, 2] JNTUA College of Engineering

Abstract- *An Artificial Neural Network (ANN) controller based series grid side converter (SGSC) scheme of doubly fed induction generator (DFIG) is presented in this paper. This proposed control methodology is utilized for compensation of grid voltage unbalances in the system and is known as the series DFIG scheme. In such DFIG scheme, the shunt connected grid side converter (GSC) is replaced by the SGSC, connected in series with the machine stator. The addition of ANN controller in the system provides low total harmonic distortion values at the point of common coupling (PCC). The proposed control methodology also exploits to compensate voltage unbalances at the point of common coupling (PCC), preventing adverse effects on loads connected next to the PCC. In this topology, the SGSC is used to control the negative sequence stator voltage to minimize the electromagnetic torque oscillations. The rotor side converter (RSC) is employed to control the negative sequence current injected through the machine stator.The validation of the proposed control topology is done by using MATLAB/SIMULINK.*

I. INTRODUCTION

Wind energy is often installed in rural, remote areas characterized by weak, unbalanced power transmission grids. In induction wind generators, unbalanced three-phase stator voltages cause a number of problems, such as over current, unbalanced currents, reactive power pulsations, and stress on the mechanical components from torque pulsations. Therefore, beyond a certain amount of unbalance, induction wind generators are switched out of the network. This can further weaken the grid. In doubly fed induction generators (DFIGs), control of the rotor currents allows for adjustable speed operation and reactive power control.A DFIG control strategy that enhances the standard speed and reactive power control with controllers that can compensate for the problems caused by an unbalanced grid voltages by balancing the stator currents are presented in.

Over the past decade, there have been significant advances in capturing wind energy using doubly fed induction generators (DFIGs).Issues pertaining to the operation and control of DFIG's subsequently became apparent, particularly in weak areas of the grid network. Ironically weak areas of the grid tend to be where the average wind speed is high and the usual location of wind farms. One of the issues that emerged was the quality of the voltage in the network at the point of common coupling (PCC) with the DFIG's. A research was undertaken into the issues of voltage unbalance and system harmonics that can deteriorate the performance of DFIGs by introducing unwanted torque harmonics and inaccuracy in the generation of commanded active/ reactive power in.

When the stator phase voltages supplied by the grid are unbalanced, the torque produced by the induction generator is not constant. Instead, the torque has periodic pulsations at twice the grid frequency, which can result in acoustic noise at low levels and at high levels can damage the rotor shaft, gearbox, or blade assembly.Also, an induction generator connected to an unbalanced voltage will draw unbalanced currents. These unbalanced currents tend to magnify the grid voltage unbalance and cause over current problems as well.Various methods for coordinating these two converters are discussed and their respective impacts on power and torque oscillations are described in.

Existing control techniques in literature to minimize the torque pulsations include: (i) rotor-side converter (RSC) compensation by supplying negative sequence voltages to the rotor circuits to suppress the negative sequence components in the rotor currents and ripples in the electromagnetic torque, or (ii) grid-side converter (GSC) compensation by compensating negative sequence currents in the grid to keep the stator currents free from negative sequence components and thus eliminate the negative sequence components in the rotor currents. In the above mentioned references, dc-link voltage ripples are not in the modeling consideration. Large ripple in the dc-link voltage ripple is however another concern under unbalanced grid conditions. To suppress the dc-link voltage ripples and at the same time to suppress the pulsations in the rotor currents and the torque, coordinated control schemes for both the RSC and GSC are proposed in.

The major disadvantages of dual sequence control include its extensive measurements, complicated computation for the reference current values and the usage of low pass filters for sequence component separation. These filters contribute excessive time delays and can deteriorate the control performance. Development and implementation of control scheme that can overcome the major shortcomings of the dual sequence control while realizing the control objectives and consideration of pulsations in the rotor currents and the torque and the ripples in the dc-link voltage are in.

A two converter series topology in which the SGSC replaces entirely the GSC functions which can avoid the additional cost of a third converter, has been proposed. To achieve this objective the DC-Link voltage control was integrated to the SGSC. This DFIG topology has allowed to combining the capacity to deal with voltage disturbances of the three-converter series topology with the lower cost of the two converters of a traditional DIFG scheme.

Although the series compensation of the series-DFIG scheme can improve the voltage unbalance levels at the PCC, so far no control strategies have been proposed for this task using this scheme. This task requires a coordinated control of the converters to inject the negative sequence current and the compensation of the torque oscillations due to these currents in the machine. To accomplish this, the present study proposes the control of the negative sequence current by the RSC, and the control of the stator voltage by the SGSC to minimize the torque oscillations. Machine learning based or Artificial Intelligence (AI)-based control architecture has been proposed to overcome some of the aforementioned issues.

In this paper, an ANN controller implemented scheme for compensating the grid voltage unbalance using series-DFIG is presented. The main objectives of the presented topology are:

a) Exploiting a new DFIG configuration, this presents the functions of a DVR without the need of an additional converter;
b) Protecting the integrity of the machine under grid voltage unbalances conditions;
c) Minimizing or even eliminating the grid voltage unbalance at the PCC, therefore preventing issues associated with loads connected to grid sensitive to voltage unbalances.

This paper is organized as follows: Section II provides the proposed configuration of the DFIG operation under unbalanced currents and the machine dynamic model which is used in Section III to show the proposed control methodology. Section IV presents the brief analysis of ANN. The validation of the proposed methodology by simulation results are presented in Section V. Finally, the main conclusions are presented in Section VI.

II. SYSTEM ARCHITECTURE AND MODEL

When conventional parallel grid side converter is totally replaced by the SGSC, as shown in Fig. 1, the SGSC is in charge of controlling the stator terminal voltage, and the DC-link.The idea of SGSC is to have a controlled series voltage with the stator and the grid. In contrast to classical configuration of wind turbine based on the DFIG, a series grid side converter and a three phase injection transformer are added in this configuration. The addition of the SGSC as a third converter in the traditional DFIG topology has demonstrated to enhance the limit of the DFIG to react to voltage sags, swells and faults in the grid, since it empowers controlling the stator terminal voltage by varying the output voltage of SGSC. In the series-DFIG scheme presented in Fig. 1, the SGSC is coupled to the grid by a series transformer and the DFIG operational principles remain the same. As the current flowing through the SGSC and through the stator machine are the same, or corresponding to the series transformer connection, the rotor power flow is controlled by the voltage at the SGSC, given by

$$P = U_{seriesd} \times I_{sd} - U_{seriesq} \times I_{sq} \qquad (1)$$

Where, $U_{seriesd}$ and $U_{seriesq}$ are the direct and quadrature components of the voltage induced by the transformer interfacing the SGSC, and I_{sd} and I_{sq} are the direct and quadrature components of the stator current.

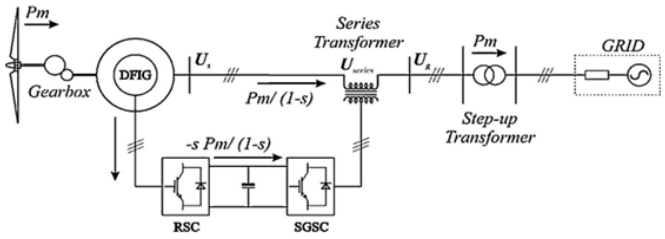

Fig. 1: Series-DFIG scheme.

The series DFIG controls under unbalanced operation conditions can be isolated in positive and negative sequences. The positive sequence variable control have the objective of controlling the active and reactive power output and the dc link voltage. For the negative sequence control, it is proposed a new control methodology.

While the negative-sequence controls proposed for the series-DFIG concentrate on controlling the output voltage

of SGSC for maintaining balanced voltages at the machine stator, in this paper it is proposed to inject an unequal current into the grid to compensate the voltage unbalance at the PCC. The series-DFIG performs more efficiently for such assignment, once the consequences of the injection of unbalanced currents can be compensated by applying a sufficient voltage at the machine stator, utilizing the SGSC. Moreover, the series-DFIG scheme permits enhancing the voltage ride through capacity.

To whole up, in the control proposed in this paper, the negative sequence control of the RSC has the target of infusing a negative sequence current through the machine, and the SGSC has the goal of forcing a voltage to the machine stator to limit the torque motions delivered by the negative sequence currents flowing through the machine. The models of the series converter and the machine are following depicted.

2.1. SGSC model

The SGSC which replaces GSC in the conventional DFIG scheme is connected in series with the stator through a series injection transformer. The SGSC is modelled as shown in the three-phase diagram of Fig. 2. A RC filter is connected in parallel to the L_c inductance to reduce the high-frequency distortions occur in the output of the three-phase IGBT bridge converter. The equivalent circuit appeared in Fig. 2(b) permits calculating the voltage in the series transformer (U_{series}) according to voltage inserted by the IGBT bridge converter (U_{sc}) and to the RLC values. It is significant that in Fig. 2(a), the series transformer is delta connected and the RC filter is star associated.

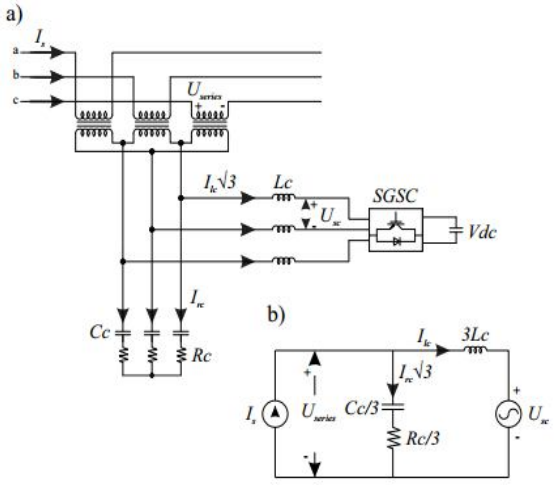

Fig. 2: (a) SGSC three-phase scheme. (b) SGSC equivalent circuit.

The compensation of unbalanced currents by the series-DFIG is implemented based on the machine symmetrical components model, which is following displayed.

Asynchronous machine dynamic model

Fig. 3 represents the T equivalent circuit of the DFIG in the positive sequence synchronous reference frame $(dq)^+$.The dq model is frequently used for modelling the wound asynchronous machine. The equations in the abc frame and the dq transformations can be obtained in. In Fig. 3, $\omega_1$is the synchronous frequency, ω_r is the rakish speed of the rotor changed over into electrical frequency and (ω_1- ω_r) is the slip frequency. Lm is the charging inductance, L_s (L_r) the stator (rotor) leakage inductance, and R_s (R_r) the stator (rotor) protection.

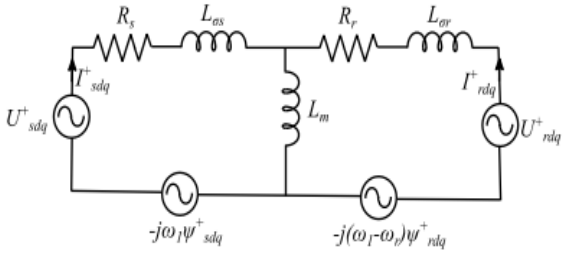

Fig. 3. DFIG equivalent circuit in the (dq)+ reference frame.

U^+_{sdq}(U^+_{rdq}), I^+_{sdq}(U^+_{rdq}) and Ψ^+_{sdq}(Ψ^+_{rdq})are the stator (rotor) voltage, current and transition alluded to the synchronous reference outline. As indicated by the proportionate circuit of the DFIG in the positive sequence synchronous reference outline, spoke to in the conditions by the superscript "+", the stator and rotor voltages can be communicated by

$$U^+_{sdq} = R_s I^+_{sdq} + \frac{d\Psi^+_{sdq}}{dt} + j\omega_1 \Psi^+_{sdq} \quad (2)$$

$$U^+_{rdq} = R_r I^+_{rdq} + \frac{d\Psi^+_{rdq}}{dt} + j(\omega_1 - \omega_r)\Psi^+_{rdq} \quad (3)$$

The motions of stator and of rotor are given by

$$\Psi^+_{sdq} = L_s I^+_{sdq} + L_m I^+_{rdq} \quad (4)$$

$$\Psi^+_{rdq} = L_m I^+_{sdq} + L_r I^+_{rdq} \quad (5)$$

Where

$$L_s = L_m + L_{os} \quad (6)$$

$$L_r = L_m + L_{\sigma r} \quad (7)$$

Ignoring the effect of R_s losses, the stator voltage can be written as

$$U_{sdq}^{+} \approx \frac{d\Psi_{sdq}^{+}}{dt} + j\omega_1 \Psi_{sdq}^{+} \quad (8)$$

According to (4), I_{sdq}^{+} can be expressed:

$$I_{sdq}^{+} = \frac{U_{sdq}^{+} - L_m I_{rdq}^{+}}{L_s} \quad (9)$$

In the equivalent circuit, the electromagnetic power is established by the sum of the exported from the voltage sources $j\omega_1 \Psi_{sdq}^{+}$ and $j(\omega_1 - \omega_r)\Psi_{rdq}^{+}$.

$$P_e = -Re[j\omega_1 \Psi_{sdq}^{+} \times \hat{I}_{sdq}^{+} + j(\omega_1 - \omega_r)\Psi_{rdq}^{+} \times \hat{I}_{rdq}^{+}] \quad (10)$$

Dealing with the fluxes and currents in the dq reference frame as complex numbers, "×" characterizes the complex product between two complex numbers and "^" the conjugate complex of a complex variable. Substituting $\hat{I}_{sdq}^{+}$ and Ψ_{rdq}^{+} by (9) and (5), respectively, it is possible to simplify (10):

$$P_e = -\omega_r \left(\left(\frac{L_m}{L_s} \right) I_m \left(\Psi_{sdq}^{+} \times \hat{I}_{rdq}^{+} \right) \right) \quad (11)$$

From P_e, the electromagnetic torque can be derived:

$$T_e = \frac{pP_e}{\omega_r} \quad (12)$$

Where, p is the number of poles of the asynchronous machine. The d axis of the dq frame is aligned to phase aof the stator voltage. Thus, the simplification $U_{sq+}^{+} = 0$ is valid and can be received in the equations.

Dynamic model of DFIG using symmetrical components

Under unequal voltage conditions, the voltages, currents and transitions of the machine can be communicated by utilizing symmetrical components. A variable F is characterized to speak to vectors communicated in the stator stationary hub organized as

$$F_{\alpha\beta}(t) = F_{\alpha\beta+}(t) + F_{\alpha\beta-}(t) \quad (13)$$

$$F_{\alpha\beta}(t) = |F_{\alpha\beta+}(t)| e^{j(\omega_1 t + \varphi_+)} + |F_{\alpha\beta-}(t)| e^{-j(\omega_1 t + \varphi_-)} \quad (14)$$

Where the subscripts "+, −" speak to the positive and negative sequence components, with "ϕ+, ϕ-" being their underlying phase shifts. Likewise, F can be re-communicated in the positive synchronous (dq)+ organize and in the negative synchronous (dq)– facilitate, demonstrated in the conditions by the superscripts "+, – ", separately, being ω1 the synchronous frequency. Subsequently, the stator vectors are decayed into:

$$F_{dq}^{+} = F_{\alpha\beta} e^{-j\omega_1 t} \quad (15)$$

$$F_{dq}^{-} = F_{\alpha\beta} e^{j\omega_1 t} \quad (16)$$

And the rotor vectors, indicated by the superscript r, as

$$F_{dq}^{+} = F_{\alpha\beta}^{r} e^{-j(\omega_1 - \omega_r)t} \quad (17)$$

$$F_{dq}^{-} = F_{\alpha\beta}^{r} e^{j(\omega_1 - \omega_r)t} \quad (18)$$

The stator/rotor conditions can be revised regarding their positive/negative sequence components in the $(dq)^{+}$ outline. The stator reference outline, communicated by the subscript s, pivots at the frequency of ω_1, and the rotor reference outline, communicated by the subscript r, turns at the frequency of $(\omega_1 - \omega_r)$,

$$F_{sdq}^{+} = F_{sdq+}^{+} + F_{sdq-}^{+} \quad (19)$$

$$F_{sdq}^{+} = F_{sdq+}^{+} + F_{sdq-}^{+} e^{-j2\omega_1 t} \quad (20)$$

$$F_{rdq}^{+} = F_{rdq+}^{+} + F_{rdq-}^{+} \quad (21)$$

$$F_{rdq}^{+} = F_{rdq+}^{+} + F_{rdq-}^{+} e^{-j2\omega_1 t} \quad (22)$$

The stator voltage can be revised in the accompanying decayed shape:

$$U_{sdq}^{+} \approx \frac{d(\Psi_{sdq+}^{+} + \Psi_{sdq-}^{-} e^{-j2\omega_1 t})}{dt} + j\omega_1 (\Psi_{sdq+}^{+} + \Psi_{sdq-}^{-} e^{-j2\omega_1 t}) \quad (23)$$

$$U_{sdq}^{+} \approx j\omega_1 (\Psi_{sdq+}^{+} - \Psi_{sdq-}^{-} e^{-j2\omega_1 t}) \quad (24)$$

Revamping the stator current as far as the positive/negative sequence components:

$$I_{sdq}^{+} = \frac{(\Psi_{sdq+}^{+} + \Psi_{sdq-}^{-} e^{-j2\omega_1 t})}{L_s} - \frac{L_m (I_{sdq+}^{+} + I_{sdq-}^{-} e^{-j2\omega_1 t})}{L_s} \quad (25)$$

The electromagnetic power can be decayed into a nonstop component in addition to throbbing components with frequency of $2\omega_1$. To accomplish this decay the accompanying conditions for the stator transition and rotor current must be connected in (11)

$$\Psi^{+}_{sdq} = \Psi^{+}_{sdq+} + \Psi^{-}_{sdq-} e^{-j2\omega_1 t} \quad (26)$$

Where the term $e^{-j2\omega_1 t}$ can be rewritten in the sin/cos form:

$$\Psi^{+}_{sdq} = \Psi^{+}_{sdq+} + \Psi^{-}_{sdq-} (\cos(2\omega_1 t) - j\sin(2\omega_1 t)) \quad (27)$$

Similarly for the rotor current:

$$I^{+}_{rdq} = I^{+}_{rdq+} + I^{-}_{rdq-} (\cos(2\omega_1 t) - j\sin(2\omega_1 t)) \quad (28)$$

At long last, substituting (23) and (24) in (11), the disintegrated type of the electromagnetic power is acquired:

$$P_e = P_{e,dc} + P_{e,cos(2)} \cos(2\omega_1 t) + P_{e,sin(2)} \sin(2\omega_1 t) \quad (29)$$

Where the subscripts e, dc, and e, sin(2) remain for the dc component and the cosine/sine components at the frequency of $2\omega_1$. The pulsating components are characterized by

$$\begin{bmatrix} P_{e,cos(2)} \\ P_{e,sin(2)} \end{bmatrix} = -\frac{L_m \omega_r}{L_s} \begin{bmatrix} -\Psi^{-}_{sq-} & \Psi^{-}_{sd-} & -\Psi^{+}_{sq+} & \Psi^{+}_{sd+} \\ \Psi^{-}_{sd-} & \Psi^{-}_{sq-} & -\Psi^{+}_{sd+} & -\Psi^{+}_{sq+} \end{bmatrix} \begin{bmatrix} I^{+}_{rd+} \\ I^{+}_{rq+} \\ I^{-}_{rd-} \\ I^{-}_{rq-} \end{bmatrix} \quad (30)$$

By the equations of the asynchronous machine decomposed into positive/negative sequence components, it is possible to build up various objectives of controlling the positive and the negative sequence components of the machine. The proposed control for the decrease of the oscillations in the electromagnetic torque is based on the previously mentioned decomposed equations of the electromagnetic power.

III. PROPOSED CONTROL METHODOLOGY

In the proposed control topology the variables are modelled in the positive and negative sequences for controlling the RSC and the SGSC of the series-DFIG plot, and the control is performed autonomously for each sequence. The controls utilizing the variables in the positive sequence have the objective to maintain the main functions of the DFIG, which are the active and reactive power output and the dc link voltage. The controls utilizing the negative sequence of the variables are used for the negative sequence current injection and for limiting the impact of the unbalanced currents in the machine torque. These controls are following explained.

RSC

The RSC control utilizing the positive sequence variables points, as a conventional DFIG, controlling the active and reactive output power of the machine. The active power control follows the optimal relationship between the angular speed of the rotor and wind speed, and the reactive power control keeps unitary power factor. Fig. 4 represents the diagram block of positive sequence control. As can be seen in Fig. 4, the d component of the rotor positive sequence current is responsible for controlling the active output power, while the q component is responsible for controlling the reactive output power. The reference utilized is based on the stator voltage orientation. As found in Fig. 4, the measured active power of the DFIG (P(pu)) is compared with the active power of reference (P*(pu)), obtained of the aerodynamic model of the rotor, the result goes through an Artificial neural system controller (ANN controller) setting up the reference for the direct axis rotor current (I^{*}_{rd}).

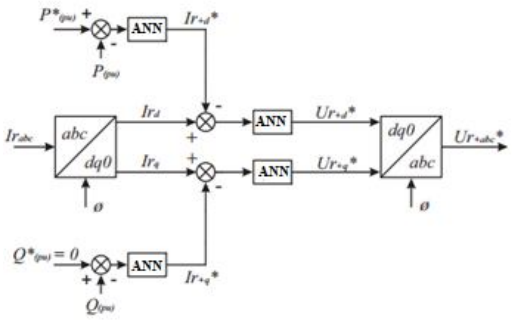

Fig. 4: Block diagram of positive sequence control of the RSC.

To set up the reference for the quadrature axis rotor current (I^{*}_{rq}), a similar procedure is applied, however utilizing the difference between the measured and reference values of the reactive power of the DFIG ($Q_{(pu)}, Q^{*}_{(pu)}$) as input the of ANN controller. The measured rotor current in the dq0 axis(I_{rd}, I_{rq}) is acquired by an abc–dq0 transformation block, and after compared with its reference values and going through an ANN controller, the reference for the positive sequence of the rotor voltage (U^{*}_{rd}, U^{*}_{rq}) is built up. A dq0–abc transformation block builds up the rotor voltage in the abc frame. The RSC negative sequence control is responsible for the negative sequence current injected by the machine stator to compensate the unbalanced grid voltage. To achieve this

target, the converter induces an unbalanced voltage at rotor windings, which will be responsible for a negative sequence current in the rotor windings and, therefore, in the stator windings too. Fig. 5 shows the block diagram of the RSC negative sequence control.

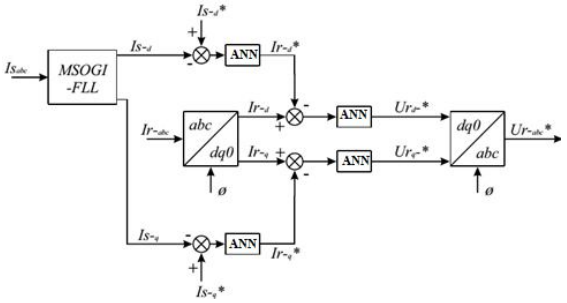

Fig. 5: Block diagram of negative sequence control of the RSC.

As can be seen by Fig. 5, the RSC negative sequence control thinks about the reference an incentive for negative sequence current of the stator (I_{s-d}^{*},I_{s-q}^{*}) with the deliberate stator negative sequence current (I_{s-d},I_{s-d}), which is acquired by a Multiple Second Order Generalized Integrator related to a Frequency Locked Loop (MSOGI-FLL). Accordingly, applying an ANN, the reference an incentive for the negative sequence rotor current (I_{r-d}^{*},I_{r-q}^{*})is acquired and, in the wake of contrasting it with the deliberate negative sequence rotor current (I_{r-d},I_{r-q}), the error goes through an ANN controller to accomplish the reference an incentive for the rotor voltage(Ur_{-d}^{*}, Ur_{-q}^{*}). The last step is the dq0– abc change block to set up the rotor voltage in the abc outline.

The reference for the negative sequence current infusion is acquired based on the equal negative sequence circuit of a straightforward transmission arrange in the synchronous reference outline pivoting at $-\omega_1$ [6]. The circuit is outlined by Fig. 6.

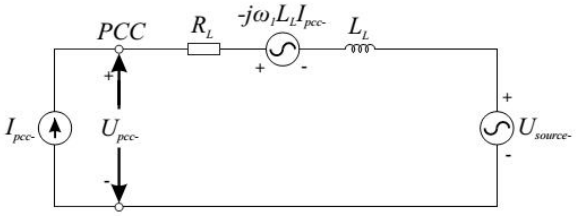

Fig. 6: Equivalent circuit of a simple transmission line rotating at −ω1.

Where, $U_{source-}$ is the negative sequence voltage before the transmission line, R_L and L_L are the equal protection and impedance of the transmission line, $I_{pcc-}$and $U_{pcc-}$are the negative sequence current and the negative sequence voltage at the point of regular coupling, individually. From Fig. 6, the voltage U_{pcc-} can be acquired:

$$U_{pcc-} = U_{source-} + R_L I_{pcc-} - j\omega_1 L_L I_{pcc-} + L_L \frac{d I_{pcc-}}{dt} \quad (31)$$

Speaking to (27) under steady state in the dq outline and disregarding the resistive voltage drop, it can be disentangled:

$$U_{pcc-d} = U_{source-d} + \omega_1 L_L I_{pcc-q} \quad (32)$$

$$U_{pcc-q} = U_{source-q} - \omega_1 L_L I_{pcc-d} \quad (33)$$

Along these lines, to repay the voltage unbalance in the point of regular coupling (U_{pcc-dq}=0), the infused negative sequence current I_{pcc-dq}can be set up:

$$I_{pcc-q} = -\frac{U_{source-d}}{\omega_1 L_L} \quad (34)$$

$$I_{pcc-d} = \frac{U_{source-q}}{\omega_1 L_L} \quad (35)$$

SGSC

The control of the SGSC utilizing the positive sequence components is responsible for controlling the DC-Link voltage. However, techniques to increase the fault-ride-through ability can also be implemented. Fig. 7 shows the block diagram of the DClink voltage control utilizing the SGSC. The control is performed by the d component of the SGSC positive sequence voltage. The q components of stator and grid voltages are kept aligned and null.

As already characterized, the negative sequence proposed control results in negative sequence currents flowing into the rotor and stator windings. These negative sequence currents cause torque oscillations, which can be removed by a particular negative sequence voltage at the SGSC.

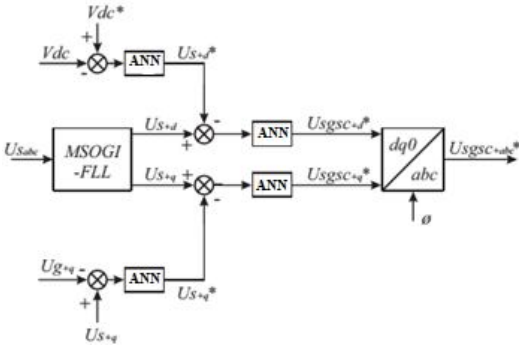

Fig. 7: Block diagram of positive sequence control of the SGSC.

To remove the pulsating components of the electromagnetic power, $P_{e,\cos 2}$ and $P_{e,\sin 2}$, the essential rotor negative sequence current should be acquired by replacing in (26) $P_{e,\cos 2}=0$ and $P_{e,\sin 2}=0$, resulting in:

$$I_{rd-}^{-} = \frac{\Psi_{sd-}}{\Psi_{sq+}^{+}} I_{rq+}^{+} - \frac{\Psi_{sd-}}{\Psi_{sq+}^{+}} I_{rd+}^{+} \quad (36)$$

$$I_{rq-}^{-} = \frac{\Psi_{sd-}}{\Psi_{sq+}^{+}} I_{rd+}^{+} + \frac{\Psi_{sq-}}{\Psi_{sq+}^{+}} I_{rq+}^{+} \quad (37)$$

As the rotor negative sequence current have been set by the RSC, it is possible to calculate the negative sequence components of the flux Ψ_{sd-}^{-} and Ψ_{sq-}^{-} adjusting (30) and (31). Utilizing the relation between the stator magnetic fluxes and the stator voltages given in (20), it is possible to compute the stator negative sequence voltage according to the rotor positive/negative sequence current to wipe out the oscillations in the torque:

$$U_{sd-}^{-} = \left(\frac{I_{rd-}^{-} I_{rd+}^{+} - I_{rq-}^{-} I_{rq+}^{+}}{I_{rd+}^{+2} + I_{rq+}^{+2}} \right) U_{sd+}^{+} \quad (38)$$

$$U_{sq-}^{-} = \left(\frac{I_{rq-}^{-} I_{rd+}^{+} + I_{rd-}^{-} I_{rq+}^{+}}{I_{rd+}^{+2} + I_{rq+}^{+2}} \right) \quad (39)$$

Applying (32) and (33) as reference for the SGSC negative sequence control the oscillations of torque must be kept in a safe level. Fig. 8 shows the block diagram of the SGSC negative sequence control. In the block diagram displayed in Fig. 8, first the negative sequence of the stator voltage at the dq reference outline is acquired. Such voltage is compared with the reference, given by (32) and (33), and the reference of negative sequence voltage for the SGSC is obtained. It is important that when the negative sequence current injection isn't required, the SGSC removes the negative sequence components of the stator voltage, maintaining a strategic distance from any torque oscillations caused by an unbalance at the machine stator.

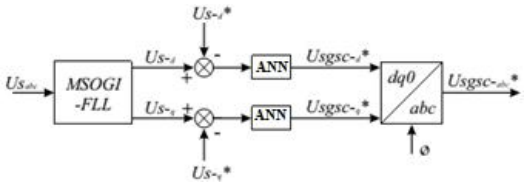

Fig. 8: Block diagram of 0 negative sequence control of the SGSC.

IV. ARTIFICIAL NEURAL NETWORKS

An artificial neural network is made of up associations of basic processing units (neurons). The essential neural network architecture comprises of an input layer, at least one center or hidden layers for processing and calculation, and an output layer. The neural network works according to the Eqn.34.

$$Y_i = \sum_{j=1}^{N} (W_{ij} X_j) \quad (40)$$

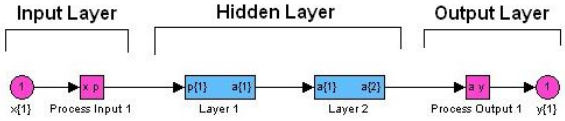

Fig. 9. Artificial Neural Network Block Diagram

The above figure 9 mimics the general piece diagram outlined using Simulink. It comprises of one input layer (process input 1), two hidden layers (layer 1, layer 2) and one output layer (process output 1).The input layer gathers information from a source. For this controller, the input information is the mistake figured by means of the feedback. Each network has just a single neuron in the principal layer on the grounds that there is just single input information esteem per side. The two hidden layers give the main computational processing (Figure 10). The main hidden layer is comprised of five neurons. The input to this layer is weighted and an inclination is included.

The activation function utilized by the principal hidden layer is a sigmoid. It determines the output activation to the second hidden layer. The second hidden layer has a single neuron and gets five inputs with weighted associations from the primary hidden layer. The inputs are summed together by this single neuron. The activation work for the second hidden layer is linear and it determines the output activation to the output layer. The output layer forms a scalar incentive to engender to the remainder of the system. After the controller interprets the information, the two ANN's create a scalar esteem each that are arrived at the midpoint of together.

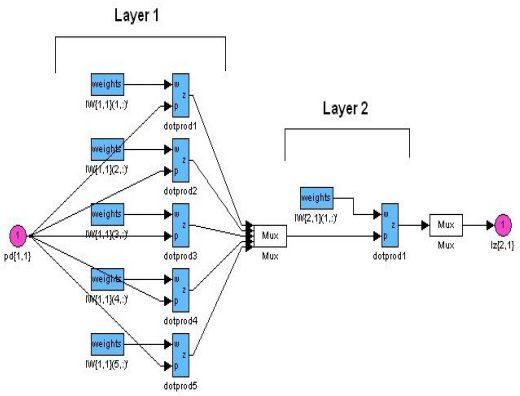

Fig. 10: Artificial Neural Network Hidden Layers

V. SIMULATION OF THE PROPOSED CONTROL STRATEGY

Simulations of the proposed control strategies of SGSC scheme for the DFIG are conducted by using Matlab/Simulink. The test system is composed by the series-DFIG, which is connected to the point of common coupling (PCC) by a transformer. A load is also connected to the PCC. A 50 km - Line connects the PCC to the 120 kV system, which is composed by a step up transformer, a mutual impedance and a 120 kV controlled voltage source. A grounding transformer is also connected to the 25 kV section to avoid zero-sequence currents flowing in the grid. The proposed system is illustrated in Fig. 11.

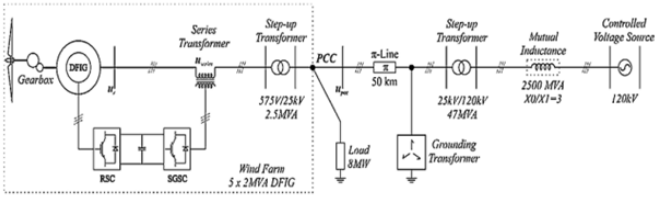

Fig. 11: Test power system configuration with DFIG.

Table 1 DFIG Data.

DFIG data		
Asynchronous generator	Rated power	2 MVA
	Rated voltage/frequency	575/60Hz
	R_s	0.023
	R_r	0.016
	L_{ls}	0.18 H
	L_{lr}	0.16 H
	Inertia constant	0.685 s
	Pair of poles	3
SGSC	L_c	0.001 H
	C_c	0.012 F
	R_c	0.5 Ω
DC link	C_{dc}	0.3 F

The DFIG rated power is 2 MVA. Its parameters are given in Table 1. In the simulations, the unbalance level is represented by the voltage unbalance factor (VUF). This index is calculated by the ratio of the negative sequence voltage with to the positive sequence voltage by [2]:

$$UVF(\%) = \frac{V_-}{V_+} . 100 \quad (41)$$

V_+ and V_- are the positive and negative sequence voltages, respectively. A VUF of 6% is imposed at the 120 kV controlled voltage source. The aim of the DFIG negative sequence injection is to compensate the voltage unbalance in the point of common coupling avoiding also the unbalance effect at the load. The operational point of the turbine for the first simulation is ω_r = 0.93 p.u. and T_m = 0.86 p.u.

The simulation of series DFIG scheme was done for following three different conditions

(i) Simulation of the DFIG for voltage unbalance in the grid with both RSC and SGSC controls enabled.
(ii) Simulation of DFIG for different angles of injected negative sequence currents.
(iii) Simulation of DFIG using only the SGSC control.

The simulation of the proposed series DFIG scheme with both PI controller and ANN controller are presented in this paper and the results are compared for both cases.

SIMULATION WITH PI CONTROL METHODOLOGY

Fig. 12 shows the point of common coupling (PCC) voltage with unbalance control enabled and disabled. Here in this case both the RSC and SGSC negative sequence controls are disabled from 0-2 sec. After 2sec, both the RSC and SGSC negative sequence controls are enabled. In the first period, the PCC presents a VUF of 4%. After enabling negative sequence current controls, the unbalance was reduced to zero.

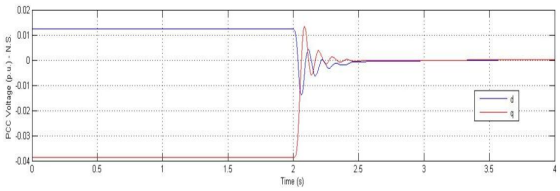

(a) Positive sequence

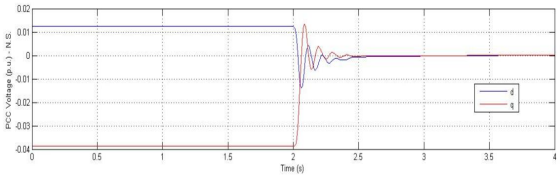

(b) Negative sequence

Fig. 12 PCC voltage (p.u.)—(a) positive sequence, (b) negative sequence.

Due to the compensation of voltage unbalance at the PCC, the negative sequence load current is also reduced. Fig. 13 shows the load current components in which the load current unbalance is almost entirely eliminated.

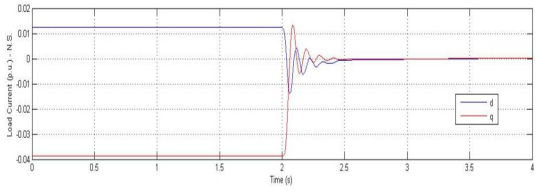

(a) Positive sequence

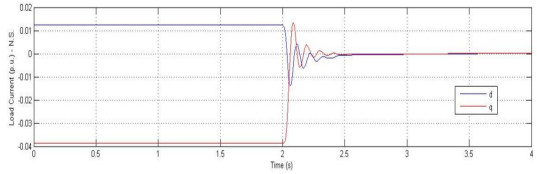

(b) Negative sequence

Fig. 13 Load current (p.u.)—(a) positive sequence, (b) negative sequence.

The RSC negative sequence control injects a negative sequence current through the stator to reduce the unbalance at the PCC. Hence, the stator current is responsible for compensating the voltage at the PCC. Fig. 14 shows the positive and negative sequence components of stator current. From this figure, the stator negative sequence current increased after the negative sequence controls enabled.

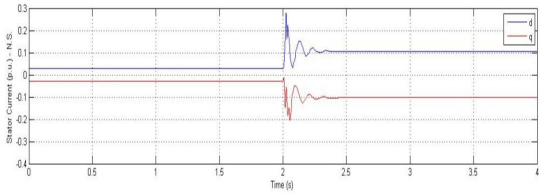

(a) Positive sequence

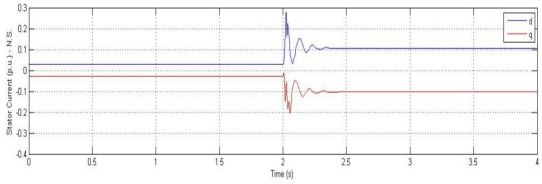

(b) Negative sequence

Fig. 14 Stator current (p.u.)—(a) positive sequence,(b) negative sequence.

The injection of negative sequence current causes the negative sequence current flowing into both rotor and stator windings. These negative sequence currents produce torque oscillations, which is eliminated by injecting a specific negative sequence voltage in series with the machine stator by SGSC. Fig. 15 illustrates the voltage at the stator terminals. The SGSC control induces a series voltage, resulting in a stator voltage that eliminates the oscillations in the electromagnetic torque, even if the machine is injecting a negative sequence current from its stator.

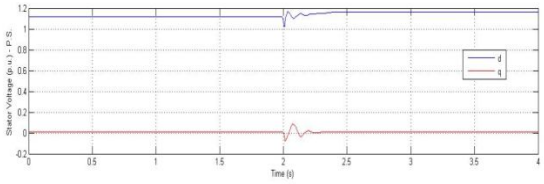

(a) Positive sequence

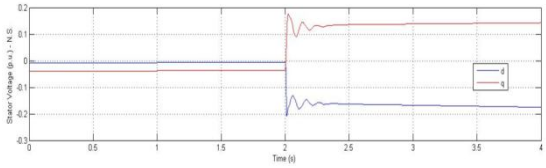

(b) Negative sequence

Fig.15 Stator voltage (p.u.) — (a) positive sequence, (b) negative sequence.

The voltage unbalance causes the electromagnetic torque oscillations at the frequency $2\omega_1$. These oscillations are

shown in the first period of Fig. 16(a). In the second period, the proposed negative sequence control for the SGSC eliminates the oscillations at the double frequency.

Fig. 16(b) shows the DFIG active power, SGSC power, and the DFIG active power. The DFIG stator active power is 0.86 p.u. and its reactive power is almost zero. In the first period the rotor power is exchanged with the RSC and SGSC positive sequence controls. In the this period, the rotor absorbs 0.12 p.u. of active power from the grid, which means that the total active power of the DFIG is 0.76 p.u. In the second period, the SGSC also absorbs active power for the negative sequence controls and the DFIG active power limits to 0.3 p.u.

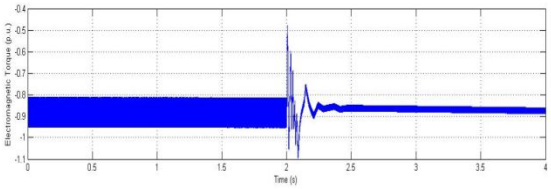

(a) Electromagnetic torque

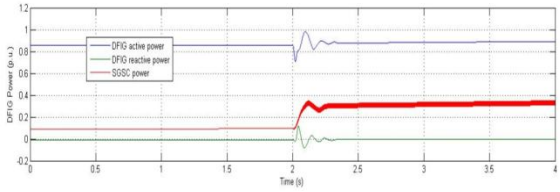

(b) DFIG Power

Fig. 16 (a) Electromagnetic torque, (b) DFIG power.

Fig. 17 shows the simulation of DFIG for different angles of the injected negative sequence stator. This can be evaluated by varying angle of grid voltage unbalance from 0^0 to 360^0 considering steps of 20^0. The SGSC control changes the stator negative sequence voltage according to the injected negative sequence current avoiding the increase in the oscillations in the electromagnetic torque.

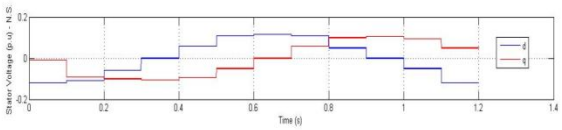

(a) Stator negative sequence voltage

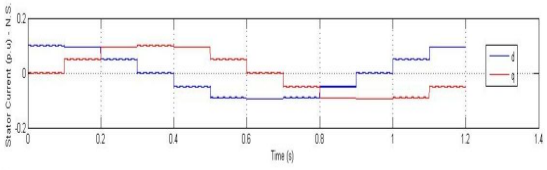

(b) Stator negative sequence current

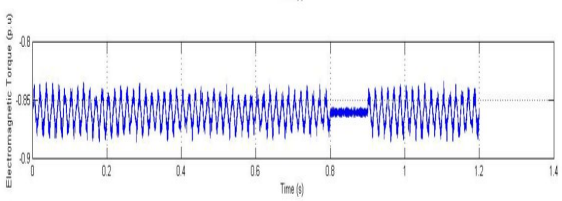

(c) Electromagnetic torque

Fig. 17 Results—current angle validation.(a) Stator negative sequence voltage (b) stator negative sequence current (c) electromagnetic torque.

Fig. 18 shows the simulation results of the series DFIG scheme with only SGSC control enabled. Fig. 18(a) presents the voltage at the machine stator. The SGSC is able to balance the voltage applied to the stator after the negative sequence control is enabled. After the voltage at the stator is balanced, the torque oscillations are reduced. Fig. 18(b) shows the electromagnetic torque waveform.

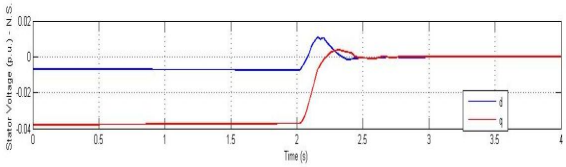

(a) Stator negative sequence voltage

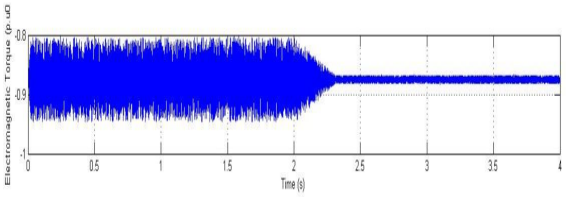

(b) Electromagnetic torque

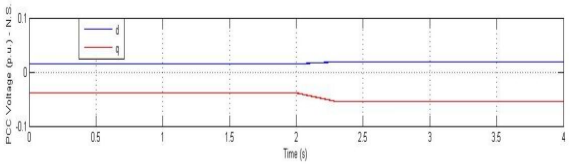

(c) PCC negative sequence voltage

Fig. 18 Stator voltage unbalance compensation (a) stator negative sequence voltage (b) electromagnetic torque (c) PCC negative sequence voltage.

SIMULATION WITH NEURAL NETWORK CONTROLLER

The simulation results of the series-DFIG scheme with neural network control methodology are shown in the following figures.

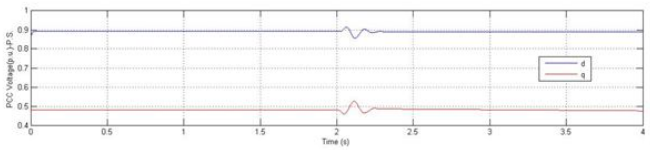

(a) Positive sequence

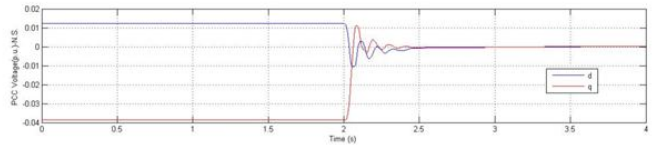

(b) Negative sequence

Fig. 19 PCC voltage (p.u.)—(a) positive sequence, (b) negative sequence.

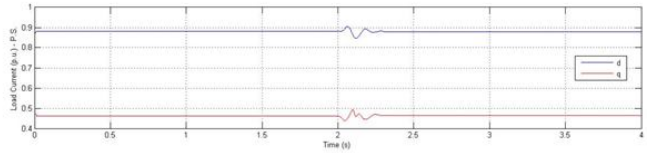

(a) Positive sequence

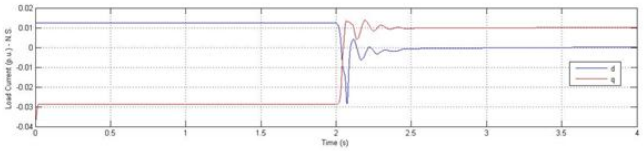

(b) Negative sequence

Fig. 20 Load current (p.u.)—(a) positive sequence, (b) negative sequence.

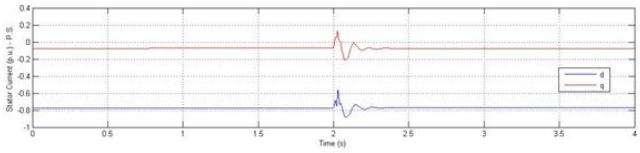

(a) Positive sequence

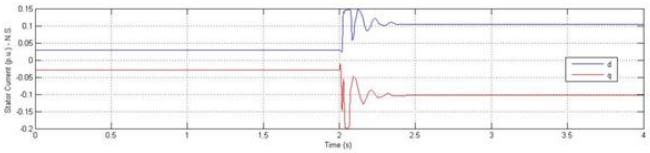

(b) Negative sequence

Fig. 21 Stator current (p.u.)—(a) positive sequence,(b) negative sequence.

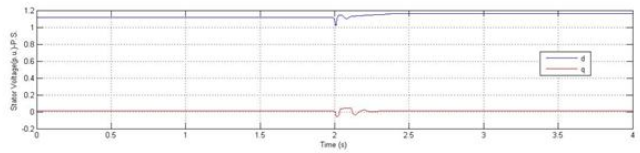

(a) Positive sequence

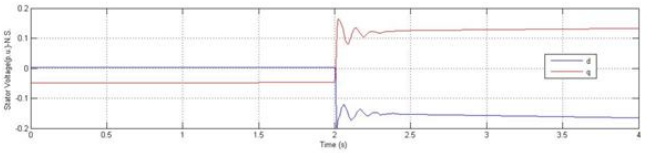

(b) Negative sequence

Fig. 22 Stator voltage (p.u.)—(a) positive sequence, (b) negative sequence.

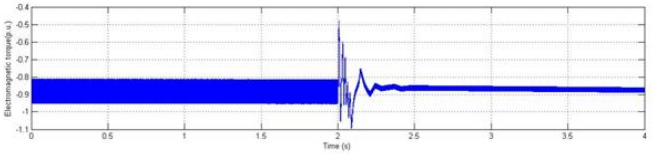

(a) Electromagnetic torque

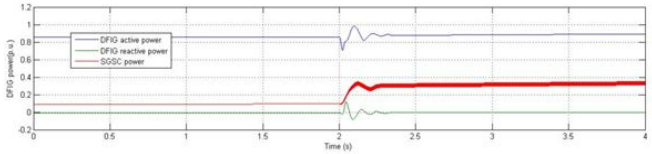

(b) DFIG Power

Fig. 23 (a) Electromagnetic torque, (b) DFIG power.

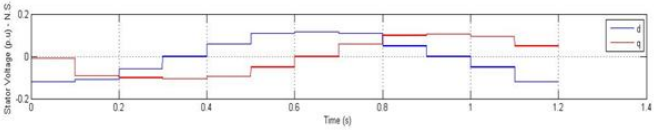

(a) Stator negative sequence voltage

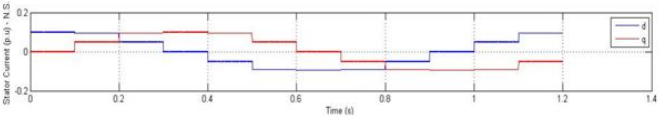

(b) Stator negative sequence current

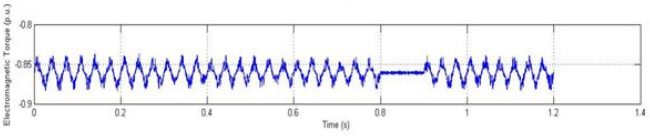

(c) Electromagnetic torque

Fig. 24 Results—current angle validation.(a) Stator negative sequence voltage (b) stator negative sequence current (c) electromagnetic torque.

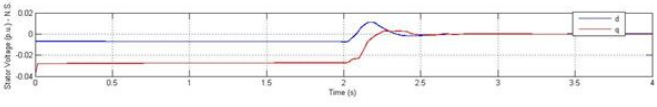

(a) Stator negative sequence voltage

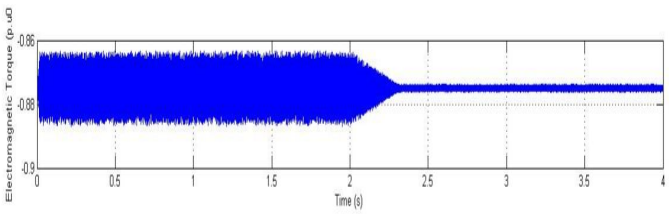

(b) Electromagnetic torque

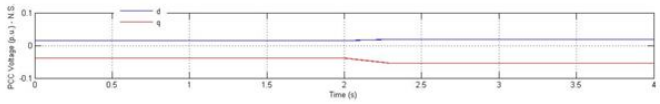

(c) PCC negative sequence voltage

Fig. 25 Stator voltage unbalance compensation (a) stator negative sequence voltage (b) electromagnetic torque (c) PCC negative sequence voltage.

The RSC negative sequence control causes the negative sequence currents to flow in the stator of the DFIG. As the results confirmed in fig. 21 that the series DFIG scheme using the neural network controller results in reduced peak overshoot in the negative sequence current compared to the control using PI controller. Also when only the SGSC control is enabled, the neural network controller results in reduced magnitude variations in the electromagnetic torque. The THD values of the voltage and currents at the point of common coupling are also shown to be reducedcompared to PI controller.

VI. CONCLUSION

In this paper, it has been proposed a control methodology with artificial neural network controller for the series-DFIG scheme for compensating the effects of voltage unbalance at the machine stator and also to reduce the total voltage unbalance at the PCC. Also the proposed methodology improves the grid voltage unbalance without compromising the machine operation. Such task was possible due to the connection of series of the grid side converter, which allows imposing a specific voltage at the machine stator to compensate the effects of the negative sequence current injected by the machine on the torque oscillations. As a result, the use of the DFIG scheme based on a series converter using the proposed ANN controller control methodology improves the penetration of the DFIG wind turbines in weak grids subjected to voltage unbalance, avoiding the propagation of the unbalance to the loads connected next to the PCC. Additionally, it is worth to highlight that other works have already demonstrated that the series-DFIG operation under grid faults have also presented good performance. As a consequence, this configuration presents a high potential to comply with more restrictive grid codes, requiring more support from the wind farm to the grid operation.

REFERENCES

[1] Y. Wang, L. Xu, B.W. Williams, Compensation of network voltage unbalance using doubly fed induction generator-based wind farms, IET Renew. Power Gener. 3 (2009) 12, http://dx.doi.org/10.1049/iet-rpg:20080007.

[2] A. von Jouanne, B. Banerjee, Assessment of voltage unbalance, IEEE Trans. Power Delivery 16 (2001) 782–790, http://dx.doi.org/10.1109/61.956770.

[3] ANSI/NEMA NEMA, Standards Publication MG1-2009: Motors and Generators, 2009.

[4] E.C. Quispe, X.M. Lopez-Fernandez, A.M.S. Mendes, A.J. Marques Cardoso, J.A. Palacios, Experimental study of the effect of positive sequence voltage on the derating of induction motors under voltage unbalance, in: 2011 IEEE Int. Electr. Mach. Drives Conf., IEEE, 2011, pp. 908–912, http://dx.doi.org/10.1109/IEMDC. 2011.5994936.

[5] J. Kearney, Grid Voltage Unbalance and the Integration of DFIG's, 2013, http://arrow.dit.ie/engdoc/56(accessed November 12, 2015) (Doctoral).

[6] M. Kiani, Effects of voltage unbalance and system harmonics on the performance of doubly fed induction wind generators, IEEE Trans. Ind. Appl. 46 (2010) 562–568, http://dx.doi.org/10.1109/TIA. 2010.2041087.

[7] H. Xu, J. Hu, Y. He, Integrated modeling and enhanced control of DFIG under unbalanced and distorted grid voltage conditions, IEEE Trans. Energy Convers. 27 (2012) 725–736, http://dx.doi.org/10.1109/TEC. 2012.2199495.

[8] T.K.A. Brekken, N. Mohan, Control of a doubly fed induction wind generator under unbalanced grid voltage conditions, IEEE Trans. Energy Convers. 22 (2007) 129–135, http://dx.doi.org/10.1109/TEC. 2006.889550.

[9] Y. Song, H. Nian, Modularized control strategy and performance analysis of DFIG system under unbalanced and harmonic grid voltage, IEEE Trans. Power Electron. 30 (2015) 4831–4842, http://dx.doi.org/10.1109/TPEL. 2014. 2366494.

[10] P. Cheng, H. Nian, Collaborative control of DFIG system during network unbalance using reduced-order generalized integrators, IEEE Trans. Energy Convers. 30 (2015) 453–464, http://dx.doi.org/10.1109/TEC. 2014.2363671.

[11] P.-H. Huang, M.S. El Moursi, S.A. Hasen, Novel fault ride-through scheme and control strategy for doubly fed induction generator-based wind turbine, IEEE Trans. Energy Convers. 30 (2015) 635–645, http://dx.doi.org/10.1109/TEC. 2014.2367113.

[12] H. Fathabadi, Control of a DFIG-based wind energy conversion system operating under harmonically distorted unbalanced grid voltage along with non-sinusoidal rotor injection conditions, Energy Convers. Manage. 84 (2014) 60–72, http://dx.doi.org/10.1016/j.enconman.2014.03.078.

[13] M. Farshadnia, S.A. Taher, Current-based direct power control of a DFIG under unbalanced grid voltage, Int. J. Electr. Power Energy Syst. 62 (2014) 571–582, http://dx.doi.org/10.1016/j.ijepes.2014.05.009.

[14] L. Xu, Y. Wang, Dynamic modeling and control of DFIG-based wind turbines under unbalanced network conditions, IEEE Trans. Power Syst. 22 (2007) 314–323, http://dx.doi.org/10.1109/TPWRS. 2006.889113.

[15] L. Fan, H. Yin, Z. Miao, A novel control scheme for DFIG-based wind energy systems under unbalanced grid conditions, Electr. Power Syst. Res. 81 (2011) 254–262, http://dx.doi.org/10.1016/j.epsr.2010.08.011.

[16] J. Hu, Y. He, L. Xu, Improved rotor current control of wind turbine driven doublyfed induction generators during network voltage unbalance, Electr. Power Syst. Res. 80 (2010) 847–856, http://dx.doi.org/10.1016/j.epsr.2009.12.010.

[17] J. Hu, Y. He, Modeling and enhanced control of DFIG under unbalanced grid voltage conditions, Electr. Power Syst. Res. 79 (2009) 273–281, http://dx.doi.org/10.1016/j.epsr.2008.06.017.

[18] E. Tremblay, A. Chandra, P.J. Lagace, Grid-side converter control of DFIG wind turbines to enhance power quality of distribution network, in: 2006 IEEE Power Eng. Soc. Gen. Meet., IEEE, 2006, p. 6, http://dx.doi.org/10.1109/PES. 2006.1709488.

[19] R. Pena, R. Cardenas, E. Escobar, J. Clare, P. Wheeler, Control strategy for a doubly-fed induction generator feeding an unbalanced grid or stand-alone load, Electr. Power Syst. Res. 79 (2009) 355–364, http://dx.doi.org/10.1016/j.epsr. 2008.07.005.

[20] J. Hu, H. Xu, Y. He, Coordinated control of DFIG's RSC and GSC under generalized unbalanced and distorted grid voltage conditions, IEEE Trans. Ind. Electron. 60 (2013) 2808–2819, http://dx.doi.org/10.1109/TIE. 2012.2217718.

[21] L. Fan, Z. Miao, Modeling and Analysis of Doubly Fed Induction GeneratorWind Energy Systems, Elsevier, Amsterdam, 2015.

[22] C.K.W. Schumacher, Active damping of flux oscillations in doublyfed ac machines using dynamic variation of the system's structure, in: Ninth Eur. Conf. Power Electron. Appl., Graz, Austria, 2001.

[23] P.S. Flannery, G. Venkataramanan, A Fault tolerant doubly fed induction generator wind turbine using a parallel grid side rectifier and series grid side converter, IEEE Trans. Power Electron. 23 (2008) 1126–1135, http://dx.doi.org/10.1109/TPEL. 2008.921179.

[24] Y. Liao, H. Li, J. Yao, K. Zhuang, Operation and control of a grid-connected DFIGbased wind turbine with series grid-side converter during network unbalance, Electr. Power Syst. Res. 81 (2011) 228–236, http://dx.doi.org/10.1016/j.epsr. 2010.09.002.

[25] B. Singh, V. Emmoji, S.N. Singh, I. Erlich, Performance evaluation of new series connected grid-side converter of doubly-fed induction generator, in: 2008 Jt. Int. Conf. Power Syst. Technol. IEEE Power India Conf., IEEE, 2008, pp. 1–8, http://dx.doi.org/10.1109/ICPST.2008.4745315.

[26] N.G. Jayanti, M. Basu, K. Gaughan, M.F. Conlon, A new configuration and control of doubly fed induction generator (UPQC-WG), in: 2008 34th Annu. Conf. IEEE Ind. Electron., IEEE, 2008, pp. 2094–2099, http://dx.doi.org/10.1109/IECON. 2008.4758280.

[27] J.R. Massing, H. Pinheiro, Design and control of doubly-fed induction generators with series grid-side converter, in: 2008 34th Annu. Conf. IEEE Ind. Electron., IEEE, 2008, pp. 139–145, http://dx.doi.org/10.1109/IECON.2008.4757942.

[28] P.C. Krause, O. Wasynczuk, S. Sudhoff, Analysis of Electric Machinery and Drive Systems, second ed., John Wiley & Sons, New York, United States, 2002.

[29] P. Kundur, Power System Stability and Control, McGraw-Hill, New York, United States, 1994.

[30] G. Abad, J. López, M. Rodríguez, L. Marroyo, G. Iwanski, Doubly Fed Induction Machine: Modeling and Control for Wind Energy Generation, first ed., John Wiley & Sons, New York, United States, 2011.

[31] J.C. Das, Power System Analysis: Short-Circuit Load Flow and Harmonics, second ed., CRC Press, Boca Raton, Forida, United States, 2011.

[32] P. Rodriguez, A. Luna, I. Candela, R. Mujal, R. Teodorescu, F. Blaabjerg, Multiresonant frequency-locked loop for grid synchronization of power converters under distorted grid conditions, IEEE Trans. Ind. Electron. 58 (2011) 127–138, http://dx.doi.org/10.1109/TIE. 2010.2042420.